Energy dependence of phenomenological optical model potentials for the ^{7}Li + ^{11}B reaction

L. Yang, C. J. Lin,* H. M. Jia, X. X. Xu, F. Yang, H. Q. Zhang, Z. H. Liu, P. F. Bao, and L. J. Sun
China Institute of Atomic Energy, P.O. Box 275(10), Beijing 102413, China
(Received 7 December 2012; revised manuscript received 18 March 2013; published 10 April 2013)

Angular distributions of ^{7}Li + ^{11}B elastic scattering were measured at $E_{\rm lab}(^{7}{\rm Li}) = 9.85$, 13.3, 18.3, 23.3, and 28.3 MeV within the angular range of $\theta_{\rm c.m.} \approx 15^{\circ}$–$80^{\circ}$. Optical model potentials have been extracted from these angular distributions and the data available in the literature at $E_{\rm lab}(^{7}{\rm Li}) = 34$ MeV and $E_{\rm lab}(^{11}{\rm B}) = 44$ MeV to study the gross influences of intricate coupling effects varying with the reaction energy. With fixed geometrical shapes, the strengths of both real and imaginary potentials show a linear decrease with increasing energy, which is different from previous observations.

DOI: 10.1103/PhysRevC.87.047601 PACS number(s): 24.10.Eq, 24.10.Ht, 25.70.Hi, 25.70.Bc

There is great interest nowadays in exploring the nuclear interactions of exotic nuclei by means of radioactive ion beams (RIBs). Recently, some progress has been made in RIB experiments; e.g., in Refs. [1–6] rather accurate data have been reported. However, owing to the limits of the beam intensity and quality, the reaction systems as well as the reaction energies studied with RIB are still limited. In view of this fact, instead of RIB, beams of weakly bound but stable projectiles like ^{6,7}Li and ^{9}Be have been widely utilized to obtain some useful information [7–9]. The nucleus-nucleus interaction potential is a basic element in the study of nuclear reactions. The phenomenological optical model potential (OMP) is widely adopted in practice, because it can be easily extracted by fitting the angular distribution of elastic scattering.

There now exists a large number of data on the elastic scattering of ^{6,7}Li projectiles over wide ranges of mass number ($A = 6$–208) of the target and energy ($E = 5$–156 MeV) [10]. A complete compilation of ^{6,7}Li OMP parameters using Woods-Saxon potentials is given in Ref. [11]. However, great variation exists in the parameters and it is very difficult to determine a systematic trend from this compilation, because the OMP is sensitive to the nuclear structures of projectile and target, especially for lighter reaction systems. Besides the phenomenological method, the microscopic double-folding model is another way to obtain the nucleus-nucleus interaction potential. However, it could not describe ^{6,7}Li elastic scattering successfully [12]. According to the Feshbach theory of the microscopic OMP [13], the dynamic polarization potential should be taken into account. Unfortunately, an accurate calculation of the dynamic polarization potential is rather complicated and requires detailed knowledge of the spectroscopic structure of two colliding nuclei [14–16]. A cluster model using double-folding technique may be an effective method to consider the structures of light and medium nuclei [17–22]. However, the double-folding procedure is constrained to the real part of the potential, while the imaginary potential still needs to be obtained by a phenomenological method.

In this work, the ^{7}Li + ^{11}B system was selected because it is a quite special system: both the projectile and the target are odd-A nuclei and have large ground-state quadrupole moments as well as presumable cluster structures. The angular distributions of elastic scattering have been measured at bombarding energies of $E_{\rm lab}(^{7}{\rm Li}) = 9.85$, 13.3, 18.3, 23.3, and 28.3 MeV within the angular range of $\theta_{\rm c.m.} \approx 15^{\circ}$–$80^{\circ}$. These angular distributions along with the data on $E_{\rm lab}(^{7}{\rm Li}) = 34$ MeV [23,24] and $E_{\rm lab}(^{11}{\rm B}) = 44$ MeV [25] were analyzed with the optical model. The phenomenological OMPs extracted from these data sets reflect the overall feature induced by the coupled-channel effects, the breakup and its subsequent effects of weakly bound ^{7}Li. Therefore, this method could avoid the complicated calculation of the dynamic polarization potential and provide a chance to understand the effects mentioned above as well as their overall changes with the reaction energy.

The experiment was performed at the HI-13 tandem accelerator of the China Institute of Atomic Energy. A natural boron (80% ^{11}B) target about 55 μg/cm^{2} thick evaporated onto a 10 μg/cm^{2}^{197}Au foil was bombarded with a ^{7}Li beam with a typical current of about 50 pnA. The Coulomb scattering on ^{197}Au was used to normalize the elastic scattering on ^{11}B. In addition, a Faraday cup was used for the absolute measurement of the beam current. These two normalization methods are consistent within error. A detector array including three Si(Au) surface barrier detectors and four $\Delta E - E$ Si(Au) telescopes at an interval of 10° was mounted on a rotatable arm to detect scattering particles. The thickness of the ΔE detectors was in the range of 20–30 μm. The other two Si(Au) detectors at $\pm 10^{\circ}$ were used to monitor the current quality. The typical energy spectrum obtained by the single Si(Au) detector is shown in Fig. 1(a). The ^{11}B elastic peak can be clearly separated from the ^{10}B one and others. Figure 1(b) shows a typical $\Delta E - E$ spectrum and the quasielastic area (shown by a square) is projected onto the energy scale, as shown in Fig. 1(c). There are almost no elastic scattering events of ^{7}Li on ^{10}B at that angle. Energy spectra were fitted by the sums of Gaussian functions with the peak positions fixed to the corresponding kinetic energies, as shown by the solid curves in the figure. Finally, the angular distributions of ^{7}Li + ^{11}B are shown in Fig. 2. The errors include statistical errors and fitting uncertainties.

*Corresponding author: cjlin@ciae.ac.cn

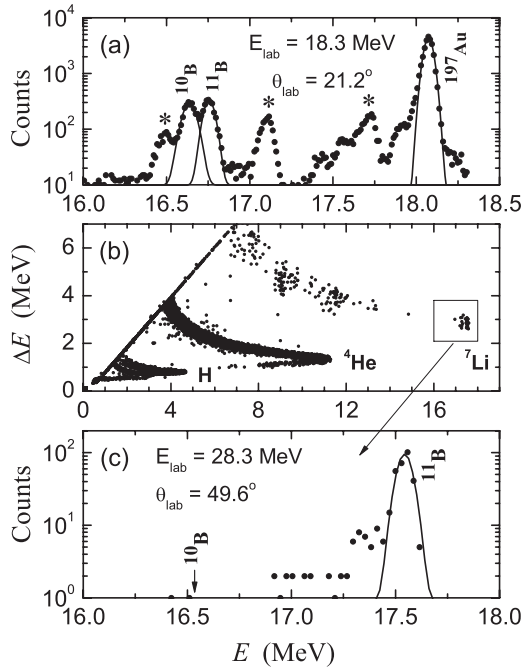

FIG. 1. (a) Typical energy spectrum for ^{7}Li + ^{11}B at $E_{\rm lab}(^{7}{\rm Li}) = 18.3$ MeV and $\theta_{\rm lab} = 21.2^{\circ}$. Peaks marked with an asterisk are from target contaminants. (b) Typical $\Delta E - E$ spectrum at $E_{\rm lab}(^{7}{\rm Li}) = 28.3$ MeV and $\theta_{\rm lab} = 49.6^{\circ}$. (c) Projection energy spectrum from the selected square in (b). Solid curves show the results of Gaussian fitting.

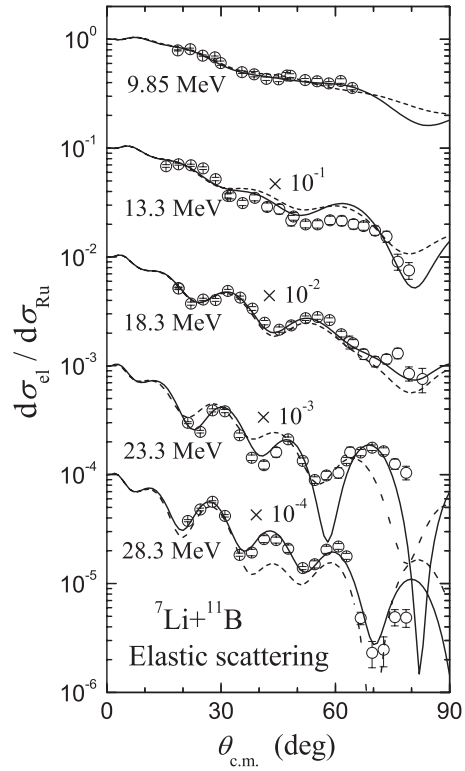

FIG. 2. Angular distributions of elastic scattering for the ^{7}Li + ^{11}B system. Open circles represent the experimental data. Best-fit results are shown by solid curves, and dashed curves show the fit results with the adopted potential shape.

The OMP can be written as the sum of the real and imaginary nuclear potentials as well as a Coulomb potential:

$$U(r) = -Vf_R(r) - iWf_I(r) + V_C(r). \quad (1)$$

The most widely used shape for the form factors $f_R(r)$ and $f_I(r)$ is the Woods-Saxon function. The spin-orbit term is not included in the potential because the polarization data were not available in this experiment. Large variations in the Coulomb radius can be compensated by minor variations in the real potential [26] without appreciable change in the quality of the fit. Thus the reduced radius, r_{0C}, was kept constant at 1.30 fm throughout the analyses.

The angular distributions of the ^{7}Li + ^{11}B elastic scattering were fitted with the PTOLEMY code [27], which can be used for heavy-ion direct reactions to extract the OMP parameters $\{X_i = V, r_{0V}, a_V, W, r_{0W}, a_W\}$; here, V and W stand for the real and imaginary parts of the volume potentials, respectively. For each angular distribution, the "goodness-of-fit" quantity was described by χ^2 analysis. The code then automatically varied the potential parameters to minimize the χ^2. First, a grid search on these six potential parameters was carried out, to obtain the best fit to the angular distributions at different bombarding energies, and the OMP parameters of ^{7}Li + ^{11}B were obtained and are listed in Table I. Then the average geometry parameters $r_{0V} = 0.93$ fm, $a_V = 0.51$ fm, $r_{0W} = 1.21$ fm, and $a_W = 0.90$ fm were extracted from the best-fit results and kept fixed to re-search the potential depths V and W. The extracted radius and diffuseness of the imaginary potential are obviously larger than those of the real potential. This might relate to the large quadrupole moments and the breakup effects, leading to absorption processes taking place at a larger distance with greater diffuseness. In Fig. 2 the theoretical angular distributions of elastic scattering with the best-fit parameters (solid curves) and the adopted geometry parameters (dashed curves) are compared with the experimental data. One finds that, although the results calculated with the adopted parameters are not as good as the best-fit results, they still describe the experimental angular distributions satisfactorily.

Besides our data, data sets taken from the literature [23,24] at $E_{\rm lab}(^{7}{\rm Li}) = 34$ MeV and the literature [25] at $E_{\rm lab}(^{11}{\rm B}) = 44$ MeV were also analyzed using the same procedure. The analysis of these two data sets was limited to the forward angle range ($\theta_{\rm c.m.} < 80^{\circ}$), but results over the whole angle range are shown in Fig. 3. The best-fit parameters are also listed in Table I. As shown in Fig. 3, the data taken from the literature [23–25] can be fitted satisfactorily for forward angles of $\theta_{\rm c.m.} < 60^{\circ}$. For backward angles, the calculated cross sections are quite oscillatory, whereas the experimental data rise smoothly towards 180°. This may be an indication of the coupling of quadrupole excitation with the entrance channel [23]. The coupled reaction channel theory could fit the entire angular range if elastic as well as inelastic scattering, reorientations of ^{7}Li and ^{11}B, and the most important one- and two-step transfers were taken into account in the channel-coupling scheme [25].

TABLE I. Best-fit parameters and adopted shapes of the OMP for ^{7}Li + ^{11}B elastic scattering.

E_{lab} (MeV)	$E_{c.m.}$ (MeV)	V (MeV)	r_{0V} (fm)	a_V (fm)	W (MeV)	r_{0W} (fm)	a_W (fm)	χ^2/pt
9.85	6.02	219.63	0.93	0.51	9.61	1.43	0.90	4.321
13.3	8.13	177.23	0.93	0.51	8.56	1.21	0.95	9.581
18.3	11.18	166.58	0.96	0.51	12.24	1.26	0.84	3.621
23.3	14.24	135.21	0.89	0.56[a]	11.32	1.11	0.92	13.64
28.3	17.29	103.99	0.93	0.51	11.67	1.28	0.73[a]	7.828
34[b]	20.78	74.96	1.07[a]	0.51	8.21	1.21	0.90	16.32
44[c]	17.13	117.61	0.93	0.51	8.15	1.21	0.90	3.539
Adopted		—	0.93	0.51	—	1.21	0.90	—

[a]These values were excluded from the calculation of average values owing to their large deviation.
[b]Experimental data are taken from Refs. [23,24].
[c]Experimental data are taken from Ref. [25]. E_{lab} is the bombarding energy of projectile ^{11}B.

For OMPs with fixed shapes, the central potential strengths can be utilized to investigate the possible energy dependence. Figure 4 shows that the depths of the real [Fig. 4(a)] and imaginary [Fig. 4(b)] potentials vary with the reaction energy, respectively. The errors on potential depths were derived by χ^2 analysis, i.e., determined by $\chi^2_{min} + 1$. One finds a concise relation between potential depth and energy. A linear function was employed to fit these data with errors as their weights. The results are as follows:

$$\begin{aligned} \{V(0) &= 261.42 \pm 9.04 - (8.98 \pm 0.46)E_{c.m.}\ \text{MeV}, \\ W(0) &= 14.62 \pm 2.82 - (0.35 \pm 0.17)E_{c.m.}\ \text{MeV}. \end{aligned} \quad (2)$$

The present results are different from those of Rudchik *et al.* [25]. They analyzed the elastic and inelastic scattering of ^{7}Li + ^{11}B with the coupled-reaction-channel method to extract the bare potentials. The energy dependence of all six parameters were fitted with exponential forms. As mentioned above, a better fit could be obtained with the coupled-reaction-channel method over a large angle range, especially forbackward angles, where the scattering is not pure potential scattering. However, this feature of the scattering would not be observed if only forward-angle data were taken [28]. Generally, OMPs for scattering from light target nuclei are more likely to show fluctuations in the parameters owing to nuclear structure and channel-coupling effects [28]. In the present work, the phenomenological OMPs extracted from

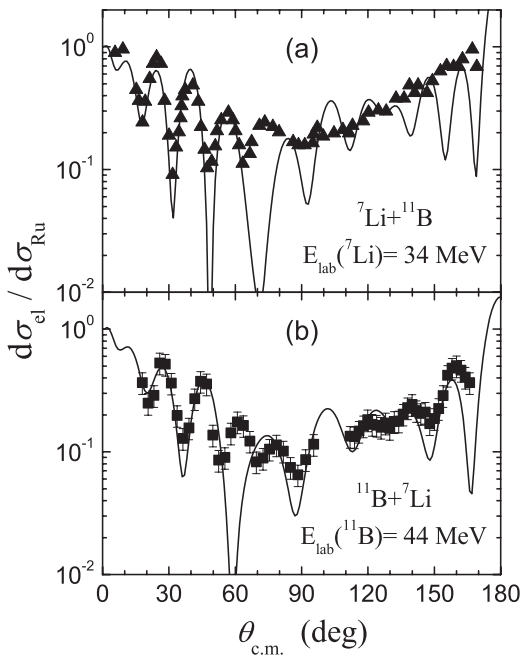

FIG. 3. Angular distributions of ^{7}Li + ^{11}B elastic scattering at bombarding energies of (a) $E_{lab}(^{7}\text{Li}) = 34$ MeV [23,24] and (b) $E_{lab}(^{11}\text{B}) = 44$ MeV [25] (b). Solid curves show the fit results with the adopted potential shape for $\theta_{c.m.} < 80^{\circ}$.

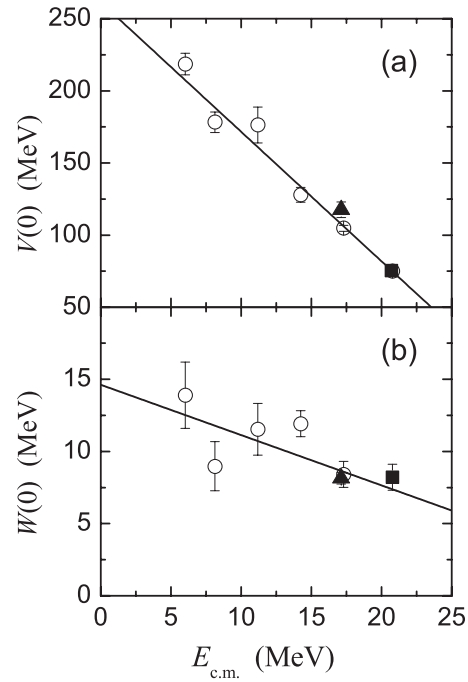

FIG. 4. Depths of (a) real and (b) imaginary potentials vary with the reaction energy for the ^{7}Li + ^{11}B system. Open circles, filled triangles, and filled squares represent results extracted from the present work, data at $E_{lab}(^{7}\text{Li}) = 34$ MeV [23,24], and data at $E_{lab}(^{11}\text{B}) = 44$ MeV [25], respectively. Solid lines show the results of linear fits with errors as weights.

the data at forward angles are not the bare but effective ones, which include all the coupling effects and related dynamical effects. Simple linear relations were found between the depths and the reaction energies when the geometric shapes were fixed. This is worthy of investigation over a wider energy range to observe the tendency. Such research may provide a valuable clue to exploration of the systematics of OMPs for light-nucleus systems and also for exotic-nucleus systems.

In summary, the angular distributions of ^{7}Li and ^{11}B elastic scattering at bombarding energies $E_{\rm lab}(^{7}{\rm Li}) = 9.85$, 13.3, 18.3, 23.3, and 28.3 MeV within the angular range of $\theta_{\rm c.m.} \approx 15^{\circ}$–$80^{\circ}$ were measured. The best-fit parameters of phenomenological OMPs were extracted and an average potential shape was adopted to further study the energy dependence of potential strengths. Data for ^{7}Li and ^{11}B elastic scattering at energies of $E_{\rm lab}(^{7}{\rm Li}) = 34$ MeV [23,24] and $E_{\rm lab}(^{11}{\rm B}) = 44$ MeV [25] were also analyzed with the adopted geometrical shape. A concise relation between potential strengths and reaction energies was obtained; i.e., the depths of real and imaginary potentials decrease linearly with increasing energy. A comprehensive investigation is strongly desirable to obtain the systematic OMPs and a better understanding of the underlying physics.

This work was supported by the National Key Basic Research Program of China under Grant No. 2013CB834404 and the National Natural Science Foundation of China under Grant Nos. 11005154, 11005156, and 11075216.

[1] M. Milin, S. Cherubini, T. Davinson *et al.*, Nucl. Phys. A **730**, 285 (2004).
[2] O. R. Kakuee, M. A. G. Alvarez, M. V. Anders *et al.*, Nucl. Phys. A **765**, 294 (2006).
[3] E. A. Benjamin, A. Lépine-Szily, D. R. Mendes, Jr. *et al.*, Phys. Lett. B **647**, 30 (2007).
[4] Y. Kucuk, I. Boztosun, and T. Topel, Phys. Rev. C **80**, 054602 (2009).
[5] A. Di Pietro, V. Scuderi, A. M. Moro *et al.*, Phys. Rev. C **85**, 054607 (2012).
[6] M. Cubero, J. P. Fernandez-Garcia, M. Rodriguez-Gallardo *et al.*, Phys. Rev. Lett. **109**, 262701 (2012).
[7] F. Michel and S. Ohkubo, Phys. Rev. C **72**, 054601 (2005).
[8] N. Keeley, K. W. Kemper, O. Momotyuk, and K. Rusek, Phys. Rev. C **77**, 057601 (2008).
[9] A. S. Denikin, P. Descouvemont, and V. I. Zagrebaev, AIP Conf. Proc. **1224**, 118 (2010).
[10] J. Cook, Nucl. Phys. A **388**, 153 (1982).
[11] J. Cook, Atom. Data Nucl. Data Tables **26**, 19 (1981).
[12] M. El-Azab Farid and M. A. Hassanain, Nucl. Phys. A **697**, 183 (2002).
[13] H. Feshbach, Ann. Phys. (NY) **5**, 357 (1985).
[14] V. Lapoux, N. Alamanos, F. Auger *et al.*, Phys. Rev. C **66**, 034608 (2002).
[15] Y. Sakuragi, Phys. Rev. C **35**, 2161 (1987).
[16] M. E. Brandan and G. R. Satchler, Phys. Rep. **285**, 143 (1997).
[17] M. E. Farid, Phys. Rev. C **65**, 067303 (2002).
[18] B. Buck, C. B. Dover, and J. P. Vary, Phys. Rev. C **11**, 1803 (1975).
[19] Y. Goto and H. Horiuchi, Prog. Theor. Phys. **62**, 662 (1979).
[20] M. El-Azab Farid, J. Phys. G **16**, 461 (1990).
[21] M. E. Farid, Z. M. M. Mahmoud, and G. S. Hassan, Phys. Rev. C **64**, 014310 (2001).
[22] M. El-Azab Farid, Z. M. M. Mahmoud, and G. S. Hassan, Nucl. Phys. A **691**, 671 (2001).
[23] J. Cook, M. N. Stephens, and K. W. Kemper, Nucl. Phys. A **466**, 168 (1987).
[24] J. Cook, A. K. Abdallah, M. N. Stephens, and K. W. Kemper, Phys. Rev. C **35**, 126 (1987).
[25] A. A. Rudchik *et al.*, Phys. Rev. C **72**, 034608 (2005).
[26] G. Bassani *et al.*, Nucl. Phys. A **189**, 353 (1972).
[27] M. Rhoades-Brown, M. H. Macfarlane, and S. C. Pieper, Phys. Rev. C **21**, 2417 (1980).
[28] M. F. Vineyard, J. Cook, K. W. Kemper, and M. N. Stephens, Phys. Rev. C **30**, 916 (1984).